Journal of Materials Chemistry

Cite this: J. Mater. Chem., 2012, 22, 17792

www.rsc.org/materials

PAPER

Synthesis and physical properties of *meta*-terphenyloxadiazole derivatives and their application as electron transporting materials for blue phosphorescent and fluorescent devices†

Cheng-An Wu,[ab] Ho-Hsiu Chou,[a] Cheng-Hung Shih,[a] Fang-Iy Wu,[a] Chien-Hong Cheng,*[a] Heh-Lung Huang,[b] Teng-Chih Chao[b] and Mei-Rurng Tseng[b]

Received 25th May 2012, Accepted 29th June 2012
DOI: 10.1039/c2jm33376g

Two *m*-terphenyloxadiazole-based electron transporting materials, bis(2-*tert*-butyl-1,3,4-oxadiazole-5-diyl)-3,3′-*m*-terphenyl (*t*OXD-*m*TP) and bis(2-(4-*tert*-butylphenyl)-1,3,4-oxadiazole-5-diyl)-3,3′-*m*-terphenyl (*t*pOXD-*m*TP) were synthesized and characterized. These two molecules contained two oxadiazolyl groups and a *m*-terphenyl linkage as the core structure achieving high triplet energy gaps (E_T) of 2.83 and 2.90 eV, respectively. The application of *t*OXD-*m*TP and *t*pOXD-*m*TP as the electron transporting materials (ETM) in bis(4′,6′-difluorophenylpyridinato)-iridium(III) picolinate (FIrpic)-based blue phosphorescent light-emitting devices effectively confines the triplet exciton in the emitting layers. One of the electroluminescent (EL) devices using FIrpic as the dopant showed an excellent current efficiency of 43.3 cd A^{-1} and an external quantum efficiency (EQE) of 23.0% with CIE (Commission International de l'Eclairage) coordinates of (0.13, 0.29). The bis(4′,6′-difluorophenylpyridinato)-iridium(III) tetra(1-pyrazolyl)borate (FIr6)-based deeper blue EL device exhibited a high current efficiency of 42.5 cd A^{-1} and external quantum efficiency of 25.0% with CIE coordinates of (0.14, 0.23). These two *t*OXD-*m*TP and *t*pOXD-*m*TP based devices show device efficiencies two to three times higher than that based on the well-known electron transporting material 1,3-bis[(4-*tert*butylphenyl)-1,3,4-oxadiazolyl]phenylene (OXD-7).

1. Introduction

Organic light emitting diodes (OLEDs) have been extensively studied for application in displays and lighting. The devices based on phosphorescent emitters benefit from the ability to harvest both singlet and triplet excitons leading to an internal quantum efficiency as high as 100%.[1] In the design of highly efficient phosphorescent devices, the selection of a proper electron transporting material (ETM) is of great importance. Due to the fact that the triplet exciton of the dopant or host material generally has a long diffusion length to the adjacent layer, the ETM should have a sufficient triplet state energy gap (E_T) to prevent the diffusion to the electron transporting layer (ETL).[2] In addition, the lowest unoccupied molecular orbital (LUMO) of the ETM should be low enough for the conducting electron to readily move from the electron injection layer and the highest occupied molecular orbital (HOMO) should also be low enough to block the hole transport. Generally, the hole mobility of hole transporting material is several orders greater than electron mobility of the electron transporting material in a device. Hence the balance of hole and electron in a device is another important issue to be considered.[3]

The requirement of ETM for blue phosphorescent electroluminescent devices is of particular importance. In addition to a large triplet energy gap and very low HOMO level, the material should have a relatively high glass transition temperature (T_g). Several types of ETM are known to date. Recently, Kido's group reported a series of pyridine derivatives as ETMs to confine the triplet excitons for sky-blue bis(4′,6′-difluorophenylpyridinato)-iridium(III) picolinate (FIrpic)-based devices. The device external quantum efficiencies (EQEs) are near or over 20%. The E_T of these pyridine-type materials is 2.6–3.0 eV. The second pyridine type of ETM is bipyridyl triazole-based materials, these also show good thermal stability and device performance.[4] Other electron transporting type functional groups like phosphine oxide, phosphine sulfide,[5] quinoxaline,[6] triazine,[7] benzimidazolyl[8] and phenanthroline[9] have been reported. The oxadiazole-based materials also have a wide energy gap and are often employed as the host or electron transporting materials in

[a]*Department of Chemistry, National Tsing Hua University, Hsinchu 30013, Taiwan. E-mail: chcheng@mx.nthu.edu.tw; Fax: +886-3-572469; Tel: +886-3-5721454*
[b]*Material and Chemical Research Laboratories, Industrial Technology Research Institute, Chutung, Hsinchu 31040, Taiwan*

† Electronic supplementary information (ESI) available: The UV-vis absorption and fluorescence data; ^{1}H, ^{13}C-NMR spectra; crystallographic information file of *t*OXD-*m*TP. CCDC 883144. For ESI and crystallographic data in CIF or other electronic format see DOI: 10.1039/c2jm33376g

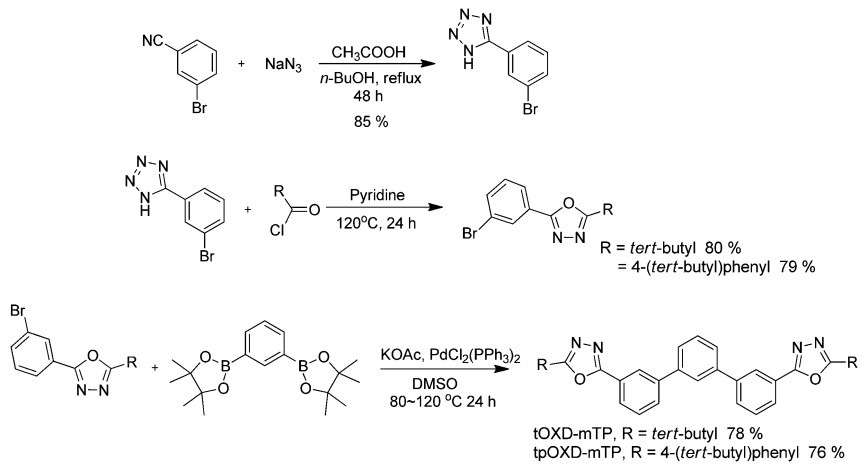

Scheme 1 Synthesis of *m*-terphenyl oxadiazole derivatives *t*OXD-*m*TP and *t*pOXD-*m*TP.

OLEDs.[10] In this series, 1,3-bis[(4-*tert*butylphenyl)-1,3,4-oxadiazolyl]phenylene (OXD-7) is very commonly used in device fabrication.[11] However, the glass transition temperature of OXD-7 is low and the triplet state energy gap of OXD-7 is not large enough for the triplet exciton confinement in deeper blue EL devices. Thus, it is a challenge to design oxadiazole-based ETMs with a larger E_T than that of OXD-7 and yet also having a high glass transition temperature. In this paper, we wish to report the synthesis of two *meta*-terphenyloxadiazole derivatives *t*OXD-*m*TP and *t*pOXD-*m*TP. These materials show higher T_g and E_T than OXD-7. It appears that the combination of *meta*-terphenyl and oxadiazole moieties is able to keep the triplet energy gap at very high values. The application of these compounds as the ETM for phosphorescent blue devices achieves excellent device performance, even with the deeper blue dopant bis(4′,6′-difluorophenylpyridinato)-iridium(III) tetra(1-pyrazolyl)borate (FIr6). Moreover, the materials can also be used as the ETM for deep blue fluorescent electroluminescent devices with excellent efficiencies.

2. Results and discussion

2.1 Synthesis and crystal structure

Scheme 1 shows the synthetic steps for the preparation of the *meta*-terphenyloxadiazole derivatives, *t*OXD-*m*TP and *t*pOXD-*m*TP. 5-(3-Bromophenyl)-1*H*-tetrazole was prepared by heating the corresponding aryl nitrile with NaN_3 and acetic acid in refluxing *n*-butanol for two days. Then the tetrazole and pivaloyl chloride was refluxed in the presence of pyridine for 24–48 h to obtain the (bromophenyl)(*tert*-butyl)oxadiazole intermediate.[12] Similarly, the (bromophenyl)(*tert*-butylphenyl)oxadiazole intermediate was obtained by using the corresponding reagents. In the last step, (bromophenyl)(*tert*-butyl)oxadiazole and (bromophenyl)(*tert*-butylphenyl)oxadiazole were treated with 1,3-phenylenediboronate under Suzuki-type cross-coupling conditions to give *t*OXD-*m*TP and *t*pOXD-*m*TP, respectively, in good yields. These compounds were characterized by ^{1}H-NMR, ^{13}C-NMR and DEPT spectroscopy, mass spectrometry and elemental analysis. In addition, the molecular structure of *t*OXD-*m*TP was determined by single-crystal X-ray crystallographic analysis.[13]

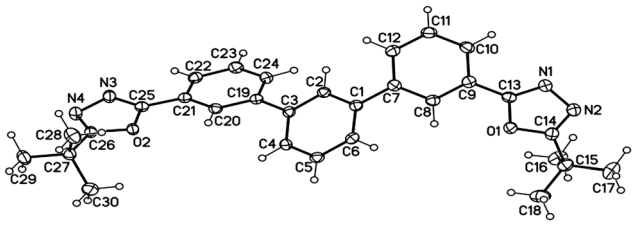

Fig. 1 The ORTEP drawing of *t*OXD-*m*TP.

As shown in Fig. 1, the dihedral angles between the first and second and second and third *m*-phenylenes in the terphenyl group are 48° and 32° indicating substantial disruption of the conjugation between the aromatic rings.

2.2 Thermal properties

The thermal properties of *t*OXD-*m*TP and *t*pOXD-*m*TP were investigated by thermal gravimetric analysis (TGA) and differential scanning calorimetry (DSC). The decomposition temperatures (T_d, corresponding to 5% weight loss) of *t*OXD-*m*TP and *t*pOXD-*m*TP were 328 and 416 °C, respectively. The T_d value of

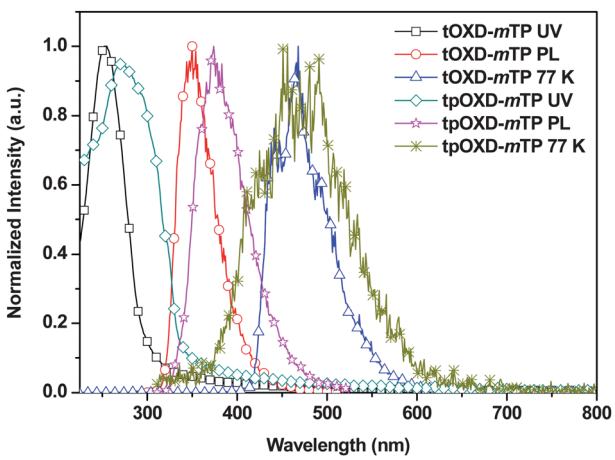

Fig. 2 The UV-vis absorption and fluorescence spectra of the thin film (30 nm) on quartz.

*t*OXD-*m*TP is close to that of OXD-7 of 330 °C, but *t*pOXD-*m*TP appears to have a much higher T_d, likely due to the presence of two extra phenyl rings in *t*pOXD-*m*TP. Similar to the trend of T_d, the glass transition temperature (T_g) of *t*pOXD-*m*TP (107 °C) is larger than that of *t*OXD-*m*TP (63 °C). However, the T_g of OXD-7 was not detected by the DSC measurement. The higher T_d and T_g of *t*pOXD-*m*TP are apparently due to the presence of two extra rigid phenyl rings and its larger molecular size compared with *t*OXD-*m*TP.

2.3 Photophysical properties

The absorption and photoluminance of terphenyloxadiazole structures in thin film and solution were analyzed by UV-vis and photoluminescence (PL) measurements as shown in Fig. 2. These materials exhibited absorption bands of 250–330 nm assigned to π–π* transitions of the oxadiazole moiety.[14] The PL spectra, which were measured in dichloromethane, show a peak maximum at 341 nm for *t*OXD-*m*TP and at 345 nm for *t*pOXD-*m*TP. The thin-film PL spectrum is red-shifted slightly to 347 nm for *t*OXD-*m*TP and by a larger degree to 375 nm for *t*pOXD-*m*TP. The observed mild red-shift of the PL spectrum of *t*OXD-*m*TP in the thin film relative to in solution indicated that the π–π interaction between molecules in the thin film is weak. The presence of the two *t*-butyl groups at the end of the molecules appears to play an important role to prevent strong intermolecular π–π interaction in the thin film state. On the other hand, the larger degree of red shift from 345 to 375 nm for *t*pOXD-*m*TP suggests that the aromatic chain consisting of five *m*-phenylene units and two oxadiazole moieties of the molecule has led to substantial intermolecular π–π interaction in the thin film state.

The singlet state energy gaps (E_g) of these two materials are calculated from the thresholds of the thin film UV spectra and are 3.86 and 3.65 eV, respectively. On the other hand, the triplet energy gaps were calculated from the highest-energy peak maximum of the phosphorescent spectra measured at low temperature. Both *t*OXD-*m*TP and *t*pOXD-*m*TP revealed very high triplet energy gaps of 2.83 and 2.90 eV, respectively. It is interesting to compare the energy gaps of *t*OXD-*m*TP and OXD-7 which have exactly the same molecular weight. As shown in Table 1, both the singlet and triplet energy gaps of *t*OXD-*m*TP are higher than the corresponding values of OXD-7 by 0.16 eV. A possible reason for this observation is that the *meta*-phenylene moieties in *t*OXD-*m*TP disrupt very effectively the π-conjugation between the two functional groups connected to a *m*-phenylene moiety. Another reason for the observation is that *t*OXD-*m*TP shows a highly non-coplanar conformation[15] due to the sterically hindered *m*-phenylene connection in the solid state, while OXD-7 is expected to be more coplanar for the three rings centered at oxadiazolyl moiety because of the sterically more open 5-membered oxadiazolyl ring (Fig. 3). The coplanar structure of OXD-7 should lead to greater intramolecular π-conjugation and intermolecular π–π overlapping. The HOMO levels were determined by a photoelectron spectrometer and the values for *t*OXD-*m*TP and *t*pOXD-*m*TP are 6.05 and 5.83 eV, respectively. The LUMO levels were then estimated by subtracting the energy gap from the HOMO levels and the values are listed in Table 1.

To understand the electron transporting character of these compounds, three electron-only devices were fabricated. The devices consist of the following structure: ITO/BCP (10 nm)/OXDs (50 nm)/LiF (1 nm)/Al (100 nm), where BCP = 2,9-dimethyl-4,7-diphenyl-1,10-phenanthroline. The current density *versus* voltage curves (see ESI†) show that the *t*OXD-*m*TP- and *t*pOXD-*m*TP-based devices gave lower current densities than the OXD-7-based one in these three electron-only devices, likely due to the relatively non-coplanar conformation and low intermolecular π–π overlapping of these two *meta*-terphenyl compounds.

3. Performance of electroluminescent devices

In order to find the suitability of these terphenyloxadiazole derivatives as the ETMs in PhOLEDs, we fabricated devices A and B by using FIrpic as the dopant emitter, BCPO as the host,[16] and *t*OXD-*m*TP and *t*pOXD-*m*TP as the ETMs. In addition, we also fabricated device C using OXD-7 as the ETM for comparison. The devices consist of the layers: ITO/NPB (30 nm)/mCP (20 nm)/BCPO: 8% FIrpic (25 nm)/ETMs (50 nm)/LiF (1 nm)/Al (100 nm), where NPB = *N*,*N*′-di(1-naphthyl)-*N*,*N*′-diphenyl-(1,1′-biphenyl)-4,4′-diamine, mCP = *N*,*N*′-dicarbazolyl-3,5-benzene and BCPO = bis-(4-(*N*-carbazolyl)phenyl)phenyl-phosphine oxide.

As shown by the *I*–*V*–*L* curves of these three devices in Fig. 4, device A using *t*OXD-*m*TP as the electron transporting material gave a very low current density compared to devices B and C using *t*pOXD-*m*TP and OXD-7 as the electron transporting material, respectively. It is interesting to note that B and C provide a very similar current density at the same applied voltage. The low intermolecular π–π stacking of the *t*OXD-*m*TP thin film leading to low electron mobility of the layer likely

Table 1 Optical and thermal properties of *t*OXD-*m*TP and *t*pOXD-*m*TP

Compd	λ_{abs}[a,b] (nm)	λ_{fl}[b,c] (nm)	λ_{phos}[d] (nm)	E_S/E_T[e] (eV)	HOMO[f] (eV)	LUMO (eV)	T_m[g] (°C)	T_g[h] (°C)	T_d[i] (°C)
*t*OXD-*m*TP	251 (252)	341 (347)	440	3.86 2.83	6.05	2.19	181	63	328
*t*pOXD-*m*TP	288 (270)	345 (375)	423	3.65 2.90	5.83	2.18	N.D.	107	416
OXD-7	292 (290)	348 (370)	466	3.70 2.67	5.98	2.28	240	N.D.	331

[a] Absorption maxima measured in CH_2Cl_2 solution at concentration = 1×10^{-5} M. [b] Wavelengths in parentheses are for thin films with thickness of 300 nm. [c] Fluorescence maxima measured in CH_2Cl_2 solution at concentration = 1×10^{-5} M. [d] The high-energy phosphorescence maxima at 77 K in 2-methyltetrahydrofuran. [e] Estimated from the absorption threshold and high-energy emission maxima in the phosphorescence spectra. [f] Determined by a photoelectron spectrometer. [g] Melting point. [h] Glass transition temperature. [i] Decomposition point.

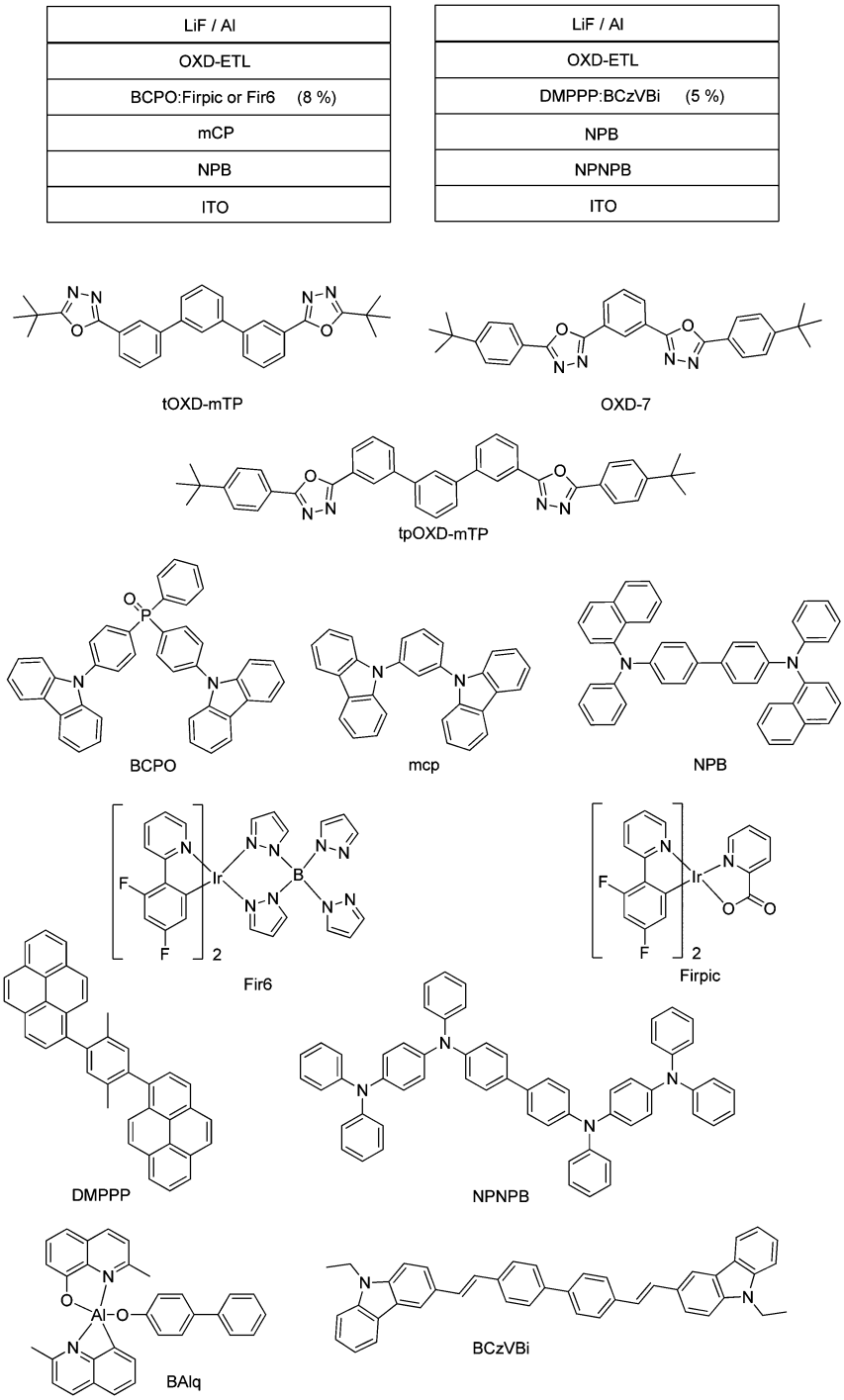

Fig. 3 The device structures and the materials structures for blue EL devices.

accounts for the very low current density of device A. The low π–π stacking of *t*OXD-*m*TP in the thin film is also supported by the very small red-shift of its emission from 341 in solution to 347 nm in the thin film of *t*OXD-*m*TP.

Devices A and B have achieved excellent EQEs of 23.0 and 20.7% with current efficiencies of 43.3 and 40.3 cd A^{-1}, respectively. However, the corresponding efficiency of the OXD-7-based device C is only about one half of the values of A and B (see Table 2). The higher efficiency of devices A and B is probably due to the fact that *t*OXD-*m*TP and *t*pOXD-*m*TP have a higher triplet energy gap to achieve better exciton confinement in the emission layer[17] and suppress the triplet exciton quenching near the emitting layer/ETL interface.[18] Device A exhibits a relatively low efficiency roll-off. At luminance of 3000 cd cm^{-2}, the EQE is maintained at more than 20% and the current efficiency is ~40 cd A^{-1}. Due to its higher ionization potential, *t*OXD-*m*TP is expected to block the holes more effectively and to enhance charge recombination in the emission layer. This blocking action

Table 2 Performances of oxadiazole-based phosphorescent OLEDs[a]

Device[b]	Host/dopant (wt%)/ETL	V_{on}[c] (V)	L (cd m^{-2}, V)	η_{ext} (%, V)	η_c (cd A^{-1}, V)	η_p (lm W^{-1}, V)	CIE, 8 V (x, y)
A	BCPO/FIrpic (8)/*t*OXD-*m*TP	3.9	13 943, 17.5	23.0, 7.0	43.3, 8.0	31.7, 4.0	0.13, 0.29
B	BCPO/FIrpic (8)/*t*pOXD-*m*TP	3.3	32 778, 18.0	20.7, 3.5	40.3, 4.0	36.2, 4.0	0.13, 0.30
C	BCPO/FIrpic (8)/OXD-7	3.9	13 280, 16.0	11.4, 5.5	22.7, 5.5	16.4, 4.0	0.18, 0.43
D	BCPO/Fir6 (8)/*t*OXD-*m*TP	4.3	13 068, 17.0	25.0, 8.0	42.5, 8.0	25.7, 4.5	0.14, 0.23
E	BCPO/Fir6 (8)/*t*pOXD-*m*TP	3.9	29 353, 17.5	20.4, 5.0	38.7, 5.0	27.7, 4.0	0.14, 0.26
F	BCPO/Fir6 (8)/OXD-7	5.1	11 147, 15.0	8.9, 9.5	14.7, 9.5	5.3, 8.5	0.14, 0.22

[a] The luminescence (L), external quantum efficiency (η_{ext}), current efficiency (η_c) and power efficiency (η_p) are the maximum values of the device. [b] The cathode of the general device is LiF (1 nm)/Al (100 nm); the structure of devices A–F: NPB (30 nm)/mCP (20 nm)/emitting layer (25 nm)/ETM (50 nm). [c] The applied voltage (V_{on}) required for a brightness of 1 cd m^{-2}.

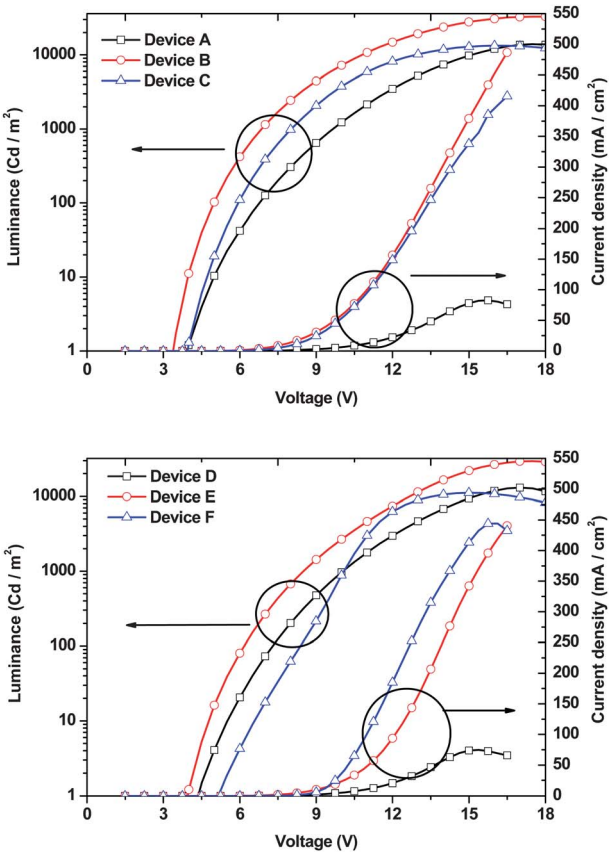

Fig. 4 The I–V–L curves of devices A–C and devices D–F.

is particularly effective at higher voltages and the roll-off is diminished.

To see the capability of these materials as an electron transporting material for deeper blue phosphorescent devices, FIr6 was chosen as the dopant for devices D–F of which the configuration is the same as that of devices A–C, respectively. Device D showed an excellent maximum EQE and current efficiency of 25.0% and 42.5 cd A^{-1}, respectively, with CIE coordinates of (0.14, 0.23) at 8 V. Device E also revealed a high external quantum efficiency and current efficiency of 20.4% and 38.7 cd A^{-1}, respectively. For comparison, device F using OXD-7 for the electron transporting layer showed an EQE of only 8.9%. The I–V–L curves of devices A–F are also shown in Fig. 4, while the EQEs and current efficiencies *vs.* luminance of these devices are displayed in Fig. 5.

To see whether *t*OXD-*m*TP and *t*pOXD-*m*TP can also be applied as the ETMs in blue fluorescent OLEDs, we fabricated devices G–J consisting of the layers: ITO/NPNPB (80 nm)/NPB (10 nm)/DMPPP: 5% BCzVBi (40 nm)/ETM (20 nm)/LiF (1 nm)/Al (100 nm), where NPNPB = *N*,*N*′-di-phenyl-*N*,*N*′-di-[4-(*N*,*N*-di-phenyl-amino)phenyl]benzidine, DMPPP = 1-(2,5-dimethyl-4-(1-pyrenyl)phenyl) pyrene and BCzVBi = 4,4′-bis(9-ethyl-3-carbazovinylene)-1,1′-biphenyl. In these devices, only the material in the electron transporting layer was varied. The device

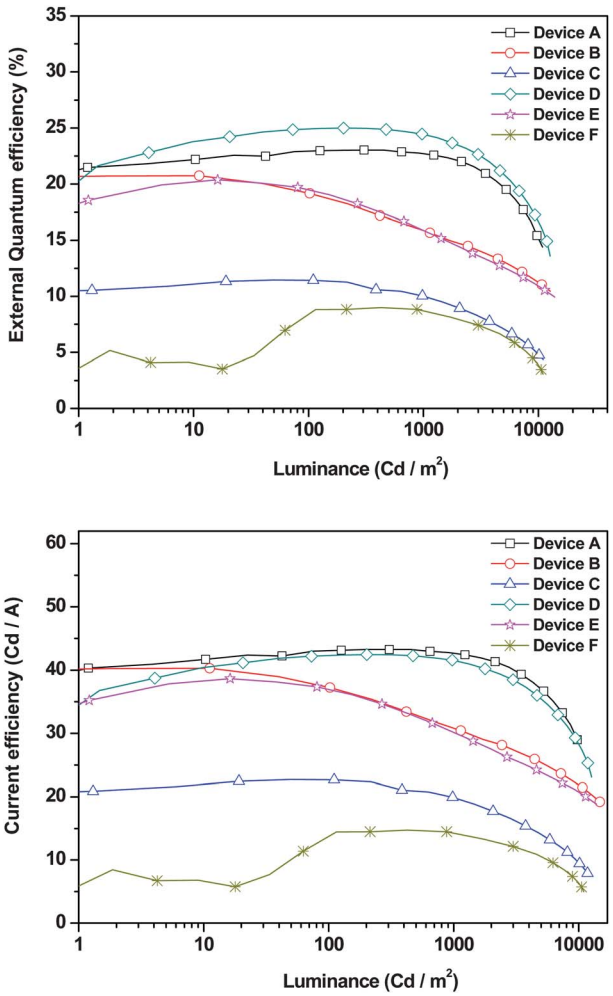

Fig. 5 External quantum efficiency and current efficiency *versus* luminance for devices A–F.

Table 3 Performances of oxadiazole-based OLEDs[a]

Device[b]	Host/dopant (wt%)/ETL	V_{on}[c] (V)	L (cd m^{-2}, V)	η_{ext} (%, V)	η_c (cd A^{-1}, V)	η_p (lm W^{-1}, V)	CIE, 8 V (x, y)
G	DMPPP/BCzVBi (5)/*t*OXD-*m*TP	4.6	14 245, 15.0	8.4, 10.5	9.9, 10.5	3.3, 8.5	0.15, 0.14
H	DMPPP/BCzVBi (5)/*t*pOXD-*m*TP	3.7	41 419, 17.5	7.3, 9.5	9.8, 10.0	4.7, 5.0	0.14, 0.16
I	DMPPP/BCzVBi (5)/OXD-7	3.7	28 825, 16.0	7.0, 10.0	8.7, 11.0	3.4, 5.5	0.15, 0.15
J	DMPPP/BCzVBi (5)/BAlq	4.9	40 694, 18.5	6.0, 13.5	8.1, 13.5	2.2, 10.5	0.14, 0.16

[a] The luminescence (L), external quantum efficiency (η_{ext}), current efficiency (η_c) and power efficiency (η_p) are the maximum values of the device. [b] The cathode of the general device is LiF (1 nm)/Al (100 nm); the structure of devices G–I: NPNPB (80 nm)/NPB (10 nm)/emitting layer (40 nm)/ETM (20 nm). [c] The applied voltage (V_{on}) required for a brightness of 1 cd m^{-2}.

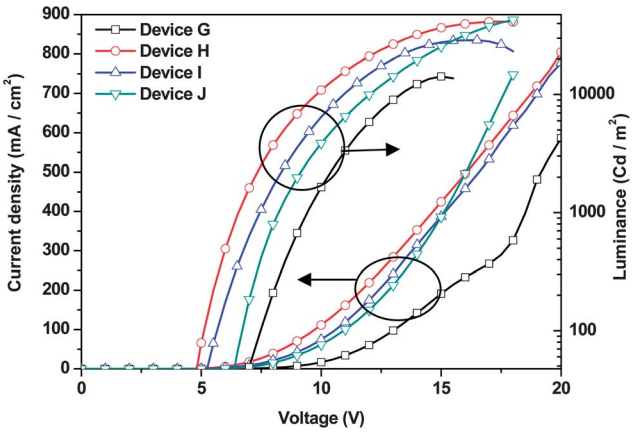

Fig. 6 The *I*–*V*–*L* curves of devices G–J.

performances are summarized in Table 3, while the *I*–*V*–*L* curves of these devices are shown in Fig. 6. Device G using *t*OXD-*m*TP as the ETM reveals the highest EQE of 8.4% (Fig. 7) and current efficiency of 9.9 cd A^{-1}, but with the smallest current density at the same applied voltage among these blue fluorescent devices G–J. Device H gave the highest current density, second highest EQE of 7.3% and the highest power efficiency of 4.7 lm W^{-1}. As expected, devices I and J using OXD-7 and BAlq as the ETM, respectively, showed lower device efficiency. The trend of the performance of these fluorescent devices is similar to that of the phosphorescent ones. The results indicate that both *t*OXD-*m*TP and *t*pOXD-*m*TP are also highly efficient ETMs for blue fluorescent devices.

4. Conclusions

Two new *meta*-terphenyl oxadiazole compounds *t*OXD-*m*TP and *t*pOXD-*m*TP were successfully synthesized and characterized. These compounds have larger triplet state energies than the well known OXD-7. The use of these *meta*-terphenyloxadiazoles as the ETMs for FIrpic and FIr6-based blue phosphorescent devices has greatly improved the device performance, *ca.* two to three times higher than that of the OXD-7-based devices. In addition, these *meta*-terphenyloxadiazoles can also be successfully applied as the ETMs for blue fluorescent devices leading to very high device efficiencies.

5. Experimental

5.1 Procedure for the synthesis of *t*OXD-*m*TP

2-(3-Bromophenyl)-5-*tert*-butyl-1,3,4-oxadiazole (5 g, 17.85 mmol), K_2CO_3 (12.31 g, 89.27 mmol), $PdCl_2(PPh_3)_2$ (10 mol%) and 1,3-bis(4,4,5,5-tetramethyl-1,3,2-dioxaborolan-2-yl) benzene (2.94 g, 8.92 mmol) and dry dimethyl sulfoxide (DMSO) (40 mL) were added to a 100 mL two-necks flask. The reaction was stirred at 80–120 °C under nitrogen until the staring material disappeared as monitored by TLC. After cooling to room temperature, the catalyst was removed by filtration and washed with chloroform. The crude product was extracted with H_2O five to six times to remove the DMSO. The organic layer was dried over $MgSO_4$, filtered and concentrated under reduced pressure and then purified by a silica gel column using a mixture of hexane and EA (2 : 1) as eluent to give the desired product in 78% yield.

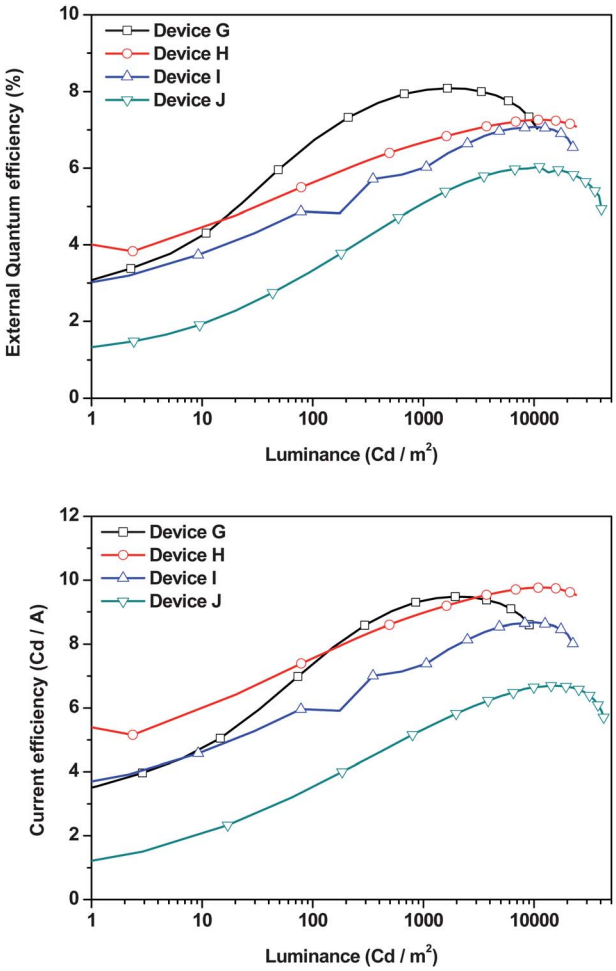

Fig. 7 External quantum efficiency and current efficiency *versus* luminance for devices G–J.

*t*pOXD-*m*TP was prepared by a procedure similar to that of *t*OXD-*m*TP. The yield is 76%.

***t*OXD-*m*TP.** ^{1}H-NMR (400 MHz, $CDCl_3$, δ): 8.31 (s, 2H), 8.05–8.03 (d, $J = 8$ Hz, 2H), 7.87 (s, 1H), 7.81–7.79 (d, $J = 8$ Hz, 2H), 7.68–7.66 (d, $J = 8$ Hz, 2H), 7.62–7.58 (m, 3H), 1.50 (s, 18H). ^{13}C-NMR (100 MHz, $CDCl_3$, δ): 173.27, 164.49, 141.85, 140.79, 130.30, 129.53, 129.50, 126.81, 126.15, 125.80, 125.47, 124.82, 32.50, 28.25; HRMS (FAB) calcd for $C_{30}H_{30}N_4O_2$ ($M^+ + 1$): 479.2447. Found: 479.2457. Anal. calcd for $C_{30}H_{30}N_4O_2$: C 75.29, H 6.32, N 11.71; found: C 75.41, H 6.41, N 11.55%.

***t*pOXD-*m*TP.** ^{1}H-NMR (400 MHz, $CDCl_3$, δ): 8.41 (s, 2H), 8.14–8.12 (d, $J = 8$ Hz, 2H), 8.09–8.07 (d, $J = 8$ Hz, 4H), 7.92 (s, 1H), 7.84–7.82 (d, $J = 8$ Hz, 2H), 7.68–7.66 (d, $J = 8$ Hz, 2H), 7.64–7.53 (m, 7 H), 1.34 (s, 18H). ^{13}C-NMR (100 MHz, $CDCl_3$, δ): 164.72, 164.20, 155.32, 141.80, 140.63, 130.35, 129.57, 129.53, 127.18, 126.75, 126.04, 125.99, 125.81, 125.51, 124.57, 120.95, 35.01, 31.04. HRMS (EI) calcd for $C_{42}H_{38}N_4O_2$ (M^+): 630.2995. Found: 630.2995. Anal. calcd for $C_{42}H_{38}N_4O_2$: C 79.97, H 6.07, N 8.88; found: C 79.77, H 6.20, N 8.87%.

5.2 Physical property measurements

UV-vis absorption spectra were recorded using a Hitachi U-3300 spectrophotometer. PL spectra and phosphorescent spectra at 77 K were measured on a Hitachi F-4500 spectrophotometer. The electrochemical properties of the OXDs derivatives were measured by Riken Keiki Co. ACII spectrometer. The HRMS were measured on a MAT-95XL HRMS or a JEOL JMS-700 Mstation. Elemental analysis was measured on an Elementar vario EL III. The glass transition temperatures of the compounds were determined by DSC under nitrogen atmosphere using a DSC-Q10 instrument. The decomposition temperatures were determined by TGA using TGA-Q500 instrument.

5.3 OLED fabrication and measurements

Organic chemicals used for fabricating devices were generally purified by high-vacuum, gradient temperature sublimation. The EL devices were fabricated by vacuum deposition of the materials at 10^{-6} Torr onto a glass precoated with a layer of indium tin oxide with a sheet resistance of 30 Ω per square. The deposition rate for organic compounds is 1–2 Å s^{-1}. The cathode consisting of Al/LiF was deposited by evaporation of LiF with a deposition rate of 0.1 Å s^{-1} and then by evaporation of Al metal with a rate of 3 Å s^{-1}. The effective area of the emitting diode was 9.00 mm^2. Current, voltage, and light intensity measurements were made simultaneously using a Keithley 2400 source meter and a Newport 1835-C optical meter equipped with a Newport 818-ST silicon photodiode. Electroluminescence spectra were measured on a Hitachi F-4500 fluorescence spectrophotometer (see ESI,† S12).

Acknowledgements

We thank the Ministry of Economy (100-EC-17-A-08-S1-042) and the National Science Council of the Republic of China (NSC-100-2119-M-007-010-MY3) for support of this research.

References

1 (*a*) M. A. Baldo, D. F. O'Brien, Y. You, A. Shoustikov, S. Sibley, M. E. Thompson and S. R. Forrest, *Nature*, 1998, **395**, 151; (*b*) M. A. Baldo, S. Lamansky, P. E. Burrows, M. E. Thompson and S. R. Forrest, *Appl. Phys. Lett.*, 1999, **75**, 4; (*c*) S. Lamansky, P. Djurovich, D. Murphy, F. Abdel-Razzaq, H. E. Lee, C. Adachi, P. E. Burrows, S. R. Forrest and M. E. Thompson, *J. Am. Chem. Soc.*, 2001, **123**, 4304; (*d*) S. Y. Ahn and Y. Ha, *Mol. Cryst. Liq. Cryst.*, 2009, **504**, 59; (*e*) C. H. Fan, P. Sun, T. H. Su and C. H. Cheng, *Adv. Mater.*, 2011, **23**, 2981; (*f*) A. Chaskar, H. F. Chen and K. T. Wong, *Adv. Mater.*, 2011, **23**, 3876; (*g*) J. Kwak, Y.-Y. Lyu, H. Lee, B. Choi, K. Char and C. Lee, *J. Mater. Chem.*, 2012, **22**, 6351.

2 (*a*) Y. Sun, N. C. Giebink, H. Kanno, B. Ma, M. E. Thompson and S. R. Forrest, *Nature*, 2006, **440**, 908; (*b*) N. Matsusue, S. Ikame, Y. Suzuki and H. Naito, *J. Appl. Phys.*, 2005, **97**, 123512; (*c*) H. Choukri, A. Fischer, S. Forget, S. Chénais, M.-C. Castex, D. Adès, A. Siove and B. Geffroy, *Appl. Phys. Lett.*, 2006, **89**, 183513; (*d*) J. Zhao, J. Yu, Z. Ma, L. Li and Y. Jiang, *Synth. Met.*, 2011, **161**, 2417; (*e*) M. Lebental, H. Choukri, S. Chénais, S. Forget, A. Siove, B. Geffroy and E. Tutis, *Phys. Rev. B: Condens. Matter Mater. Phys.*, 2009, **79**, 165318.

3 (*a*) N. Chopra, J. Lee, Y. Zheng, S.-H. Eom, J. Xue and F. So, *Appl. Phys. Lett.*, 2008, **93**, 143307; (*b*) P. Strohriegl and J. V. Grazulevicius, *Adv. Mater.*, 2002, **14**, 1439; (*c*) Y. Li, M. K. Fung, Z. Xie, S. T. Lee, L.-S. Hung, J. Shi and Y. Q. Li, *Adv. Mater.*, 2002, **14**, 1317.

4 (*a*) H. Sasabe, E. Gonmori, T. Chiba, Y.-J. Li, D. Tanaka, S.-J. Su, T. Takeda, Y.-J. Pu, K.-I. Nakayama and J. Kido, *Chem. Mater.*, 2008, **20**, 5951; (*b*) S.-J. Su, T. Chiba, T. Takeda and J. Kido, *Adv. Mater.*, 2008, **20**, 2125; (*c*) D. Tanaka, Y. Agata, T. Takeda, S. Watanabe and J. Kido, *Jpn. J. Appl. Phys.*, 2007, **46**, L117; (*d*) D. Tanaka, T. Takeda, T. Chiba, S. Watanabe and J. Kido, *Chem. Lett.*, 2007, **36**, 262; (*e*) L. X. Xiao, Z. J. Chen, B. Qu, J. X. Luo, S. Kong, Q. H. Gong and J. Kido, *Adv. Mater.*, 2011, **23**, 926; (*f*) S.-J. Su, Y. Taikahashi, T. Chiba, T. Takeda and J. Kido, *Adv. Funct. Mater.*, 2009, **19**, 1260; (*g*) M. Ichikawa, T. Yamamoto, H. Jeon, K. Kase, S. Hayashi, M. Nagaoka and N. Yokoyama, *J. Mater. Chem.*, 2012, **22**, 6765; (*h*) M. Ichikawa, S. Mochizuki, H.-G. Jeon, S. Hayashi, N. Yokoyama and Y. Taniguchi, *J. Mater. Chem.*, 2011, **21**, 11791; (*i*) M. Ichikawa, S. Fujimoto, Y. Miyazawa, T. Koyama, N. Yokoyama, T. Miki and Y. Taniguchi, *Org. Electron.*, 2008, **9**, 77.

5 (*a*) H. Tsuji, K. Sato, Y. Sato and E. Nakamura, *J. Mater. Chem.*, 2009, **19**, 3364; (*b*) S. O. Jeon, K. S. Yook, J. Y. Lee, S. M. Park, J. W. Kim, J. H. Kim, J.-A. Hong and Y. Park, *Appl. Phys. Lett.*, 2011, **98**, 073306; (*c*) A. L. Von Ruden, L. Cosimbescu, E. Polikarpov, P. K. Koech, J. S. Swensen, L. Wang, J. T. Darsell and A. B. Padmaperuma, *Chem. Mater.*, 2010, **22**, 5678.

6 (*a*) T.-H. Huang, W.-T. Whang, J. Y. Shen, Y.-S. Wen, J. T. Lin, T.-H. Ke, L.-Y. Chen and C.-C. Wu, *Adv. Funct. Mater.*, 2006, **16**, 1449; (*b*) X. Xu, G. Yu, S. Chen, C. Di and Y. Liu, *J. Mater. Chem.*, 2008, **18**, 299; (*c*) S. Dailey, W. J. Feast, R. J. Peace, I. C. Sage, S. Till and E. L. Wood, *J. Mater. Chem.*, 2001, **11**, 2238.

7 (*a*) H.-F. Chen, S.-J. Yang, Z.-H. Tsai, W.-Y. Hung, T.-C. Wang and K.-T. Wong, *J. Mater. Chem.*, 2009, **19**, 8112; (*b*) T. Matsushima, M. Takamori, Y. Miyashita, Y. Honma, T. Tanaka, H. Aihara and H. Murata, *Org. Electron.*, 2010, **11**, 16; (*c*) H. Inomata, K. Goushi, T. Masuko, T. Konno, T. Imai, H. Sasabe, J. J. Brown and C. Adachi, *Chem. Mater.*, 2004, **16**, 1285.

8 W. White, Z. M. Hudson, X. Feng, S. Han, Z.-H. Liu and S. Wang, *Dalton Trans.*, 2010, **39**, 892.

9 P. Kathirgamanathan, S. Surendrakumar, R. R. Vanga, S. Ravichandran, A.-L. Juan, S. Ganeshamurugan, M. Kumaraverl, G. Paramaswara and V. Arkley, *Org. Electron.*, 2011, **12**, 666.

10 (*a*) S. Gong, Y. Chen, X. Zhang, P. Cai, C. Zhong, D. Ma, J. Qin and C. Yang, *J. Mater. Chem.*, 2011, **21**, 11197; (*b*) S. Gong, Q. Fu, Q. Wang, C. Yang, C. Zhong, J. Qin and D. Ma, *Adv. Mater.*, 2011, **23**, 4956; (*c*) Y. Hamada, C. Adachi, T. Tsutsui and S. Saito, *Optoelectronics*, 1992, **7**, 83; (*d*) X. Yang, D. C. Müller, D. Neher and K. Meerholz, *Adv. Mater.*, 2006, **18**, 948; (*e*) A. Nakamura, T. Tada, M. Mizukami and S. Yagyu, *Appl. Phys. Lett.*, 2004, **84**, 130; (*f*) Y. Tao, C. Yang and J. Qin, *Chem. Soc. Rev.*, 2011, **40**,

2943; (*g*) X. Qiao, Y. Tao, Q. Wang, D. Ma and C. Yang, *J. Appl. Phys.*, 2010, **108**, 034508.
11 (*a*) H.-Y. Chen, C.-T. Chen and C.-T. Chen, *Macromolecules*, 2010, **43**, 3613; (*b*) T. Ye, S. Shao, J. Chen, L. Wang and D. Ma, *ACS Appl. Mater. Interfaces*, 2011, **3**, 410; (*c*) W. Jian, L. Duan, J. Qiao, D. Zhang, G. Dong, L. Wang and Y. Qiu, *J. Mater. Chem.*, 2010, **20**, 6131.
12 B. Verheyde and W. Dehaen, *J. Org. Chem.*, 2001, **66**, 4062.
13 The supplementary crystallographic data of *t*OXD-mTP is listed in CCDC-883144 respectively.
14 (*a*) C. C. Yang, C. J. Hsu, P. T. Chou, H. C. Cheng, Y. O. Su and M. K. Leung, *J. Phys. Chem. B*, 2010, **114**, 756; (*b*) P. Zhang, B. Tang, W. Tian, B. Yang and M. Li, *Mater. Chem. Phys.*, 2010, **119**, 243; (*c*) R. Mabbs, N. Nijegorodov and W. S. Downey, *Spectrochim. Acta, Part A*, 2003, **59**, 1329.
15 M.-K. Leung, C.-C. Yang, J.-H. Lee, H.-H. Tsai, C.-F. Lin, C.-Y. Huang, Y. O. Su and C.-F. Chiu, *Org. Lett.*, 2007, **9**, 235.
16 (*a*) H. H. Chou and C. H. Cheng, *Adv. Mater.*, 2010, **22**, 2468; (*b*) K. Y. Lu, H. H. Chou, C. H. Hsieh, Y. H. Ou Yang, H. R. Tsai, H. Y. Tsai, L. C. Hsu, C. Y. Chen, I. C. Chen and C. H. Cheng, *Adv. Mater.*, 2011, **23**, 4933.
17 H. Sasabe, T. Chiba, S.-J. Su, Y.-J. Pu, K.-I. Nakayama and J. Kido, *Chem. Commun.*, 2008, 5821.
18 J.-H. Lee, H.-H. Tsai, M.-K. Leung, C.-C. Yang and C.-C. Chao, *Appl. Phys. Lett.*, 2007, **90**, 243501.